NUCL SCI TECH (2017) 28:105
DOI 10.1007/s41365-017-0263-2

PL and ESR study for defect centers in 4*H*-SiC induced by oxygen ion implantation

Guo-Dong Cheng[1,2] · Ye Chen[1] · Long Yan[2] · Rong-Fang Shen[2]

Received: 10 January 2017 / Revised: 24 February 2017 / Accepted: 27 February 2017 / Published online: 29 June 2017

Abstract Radiation damage in 4*H*-SiC samples implanted by 70 keV oxygen ion beams was studied using photoluminescence and electron spin resonance techniques. ESR peak of $g = 2.0053$ and two zero-phonon lines were observed with the implanted samples. Combined with theoretical calculations, we found that the main defect in the implanted 4*H*-SiC samples was oxygen-vacancy complex. The calculated defect formation energies showed that the oxygen-vacancy centers were stable in *n*-type 4*H*-SiC. Moreover, the $V_{Si}O_C^0$ and $V_{Si}O_C^{-1}$ centers were optically addressable. The results suggest promising spin coherence properties for quantum information science.

Keywords Ion implantation · Electron spin resonance · Photoluminescence · First-principles calculations

1 Introduction

Quantum information and quantum calculation have attracted intensive attention, but a key problem hampering the progress in this area is to find suitable materials for implementing the spin qubit [1]. A negatively charged nitrogen-vacancy (NV^{-1}) center in diamond as a solid-state qubit was once studied intensively [2]. Recently, several defects in silicon carbide (SiC) were predicted to be promising candidates of spin qubit [3]. Comparing with NV^{-1} centers in diamond, the defects in SiC have much lower transition frequencies and sharp zero-phonon line (ZPL), owing to the larger lattice constant and the small overlap among the sp^3 dangling-bond orbitals. The spin coherence times of the defects in 4*H*-SiC were found to be suitable for qubit application [4]. All these encourage researches for applying the defects in SiC to the area of quantum information.

Techniques to produce defects in SiC materials include irradiation, annealing and ion implantation. Till now, several defects and complexes in SiC, such as negatively charged silicon vacancies (V_{Si}^{-1}) [5], divacancies ($V_{Si}V_C$) [3], carbon antisite–vacancy pairs (V_CC_{Si}) [6] and V_{Si}^{-1} with one neighboring carbon atom substituted by a nitrogen atom ($N_CV_{Si}^{-1}$) [7], have been produced and identified. Studies on vacancy-type defects induced by oxygen ion implantation in SiC and annealing showed evidences that new defect complex combined the vacancy-type defects with oxygen might be formed [8, 9]. However, this shall be further studied for detailed information about the defect stability, especially the spin electronic structure and optical properties. In this paper, oxygen ion-implanted 4*H*-SiC samples are implanted with 70 keV oxygen ion beams. Electron spin resonance (ESR) and photoluminescence (PL) analyses, and first-principles calculations, show that the main defect produced by oxygen ion implantation is ($V_{Si}O_C$) centers, which consist of a substitutional oxygen atom at the carbon site and an adjacent silicon vacancy in

This work was supported by the National Science Foundation of China (Nos. 61076089, 11505265 and 61227902) and the Ministry of Education of China (SRF for ROCS, SEM).

✉ Long Yan
yanlong@sinap.ac.cn

[1] Key Laboratory of Polar Materials and Devices, Ministry of Education of China, East China Normal University, Shanghai 200241, China

[2] Shanghai Institute of Applied Physics, Chinese Academy of Sciences, Jiading Campus, Shanghai 201800, China

4*H*-SiC. The spin coherence time of the $V_{Si}O_C$ centers in 4*H*-SiC is calculated using a mean-field-based scheme model. It is demonstrated that $V_{Si}O_C$ centers are suitable for qubit controlling.

2 Experimental procedure and computation method

The *n*-type 4*H*-SiC crystals were supplied by Shanghai Institute of optics and fine mechanics, the Chinese academy of sciences. The samples were implanted at room temperature by 70 keV oxygen ions to 1×10^{14} ions/cm^2. According to SRIM calculation, the implantation-induced vacancies and implanted oxygen atoms were distributed in depths of 60–160 nm. The ESR measurements were performed on a JEOL-FA200 spectrometers at 9.098-GHz (*X*-band) under standard conditions at 100–160 K. The excitation laser wavelength was 785 nm, with a laser spot of 2 μm in diameter. The PL signal was recorded by using a Bruker Raman system with 100× objective.

The linear combinations of pseudo-atomic orbitals (LCPAOs) method based on the density functional theory (DFT) were adopted in our first-principles calculations. The norm-conserving pseudopotentials were used in electron–ion interactions [10], which were treated within the generalized gradient approximation (GGA) presented by Perdew–Burke–Ernzerhof (PBE) [11]. A supercell containing 127 atoms and a silicon monovacancy were employed. A $4 \times 4 \times 4$ Monkhorst–Pack special k grid was used to the Brillouin zone integration. The atomic positions were optimized until the Hellmann–Feynman forces were less than 0.001 Ha/a.u. The characteristic *g*-value shifts of vacancy defects were calculated by the Quantum-Espresso package [12]. The spin-conserved optical transitions were calculated using the Heyd–Scuseria–Ernzerhof (HSE06) hybrid function [13], which had well reproduced the ZPL experimental values [14].

3 Results and discussion

Figure 1 shows the *X*-band ESR spectra of the pristine and oxygen ion-implanted 4*H*-SiC measured at 100–160 K. The magnetic field is parallel to the *c* axis of the crystal (B||*c*) in the measurements. No signal was detected with the pristine 4*H*-SiC measured at 100 K. After oxygen ion implantation, a very strong signal was detected with the *g* factor equals to 2.0053. This is different from the vacancy defect centers in 4*H*-SiC reported in Refs. [7, 15, 16] (V_{Si} at $g = 2.0034$, V_C at $g = 2.0038$, $V_{Si}V_C$ at $g = 2.0023$, $V_{Si}N_C$ at $g = 2.0029$ and $C_{Si}V_C$ at $g = 2.0032$), but is consistent with that of oxygen-vacancy

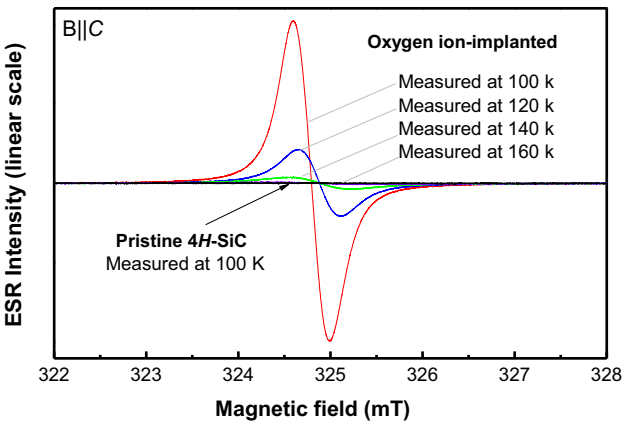

Fig. 1 (Color online) *X*-band ESR spectra measured at 100–160 K for pure and oxygen ion-implanted 4*H*-SiC. The magnetic field is parallel to the *c* axis (B||*c*)

complex in silicon ($V_{Si}O_{Si}$ at $g = 2.0057$) [17]. Figure 1also shows that ESR signals of the implanted samples decreased with increasing temperatures (disappeared at 160 K), and the peak position shifted with temperature due to the electron–phonon interaction [18].

Figure 2 shows the PL spectra of 4*H*-SiC samples measured at 100–180 K before and after ion implantation. The pristine 4*H*-SiC has just two Raman peaks, corresponding to the two inequivalence Si–C bonding configurations, while the implanted samples exhibit two sharp of ZPL peaks at 1.43 eV (866 nm) and 1.37 eV (907 nm), in addition to the two Raman peaks. The ZPL peaks decrease in height with increasing temperature (disappears at 180 K). It is well known that the ZPL peaks of the neutral $V_{Si}V_C$ center, the negatively charged state $V_{Si}N_C$ and the neutral $C_{Si}V_C$ are at 1.1 ± 0.05, 0.98 ± 0.01 and 1.0 ± 0.05 eV, respectively [3, 6, 19], and the ZPL peaks of the negatively charged state V_{Si} center are at 1.44 eV (860 nm) and 1.35 eV (917 nm) with two inequivalent

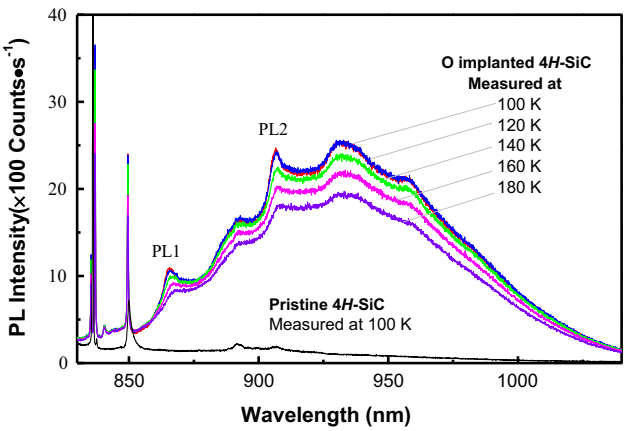

Fig. 2 (Color online) Photoluminescence spectra of oxygen ion-implanted 4*H*-SiC measured at 100–180 K

sites [5]. The ZPL peaks of the oxygen ion-implanted 4*H*-SiC differ from those vacancy defect centers and the V_{Si} center in 4*H*-SiC. These indicate that the oxygen ion implanted in 4*H*-SiC introduces new defect centers.

Generally, implantation mainly produces vacancy-type defects [16, 20]. To study these defects in 4*H*-SiC produced by oxygen ion implantation, the calculation of formation energies for all types of vacancy defects is necessary. The defect formation energy (E^f) depends on the defect charge states (q) and Fermi level (ε_F). For $V_{Si}O_C$ in 4*H*-SiC, the E^f can be extracted from the total energies via first-principle calculations [21]:

$$E^f\left(V_{Si}O_C^q\right) = E_{tot}\left(V_{Si}O_C^q\right) - E_{tot}(SiC) - \mu_O + \mu_{SiC} + q(\varepsilon_F + \varepsilon_v + \Delta V)$$

where $E_{tot}(SiC)$ and $E_{tot}\left(V_{Si}O_C^q\right)$ are the total energies of the perfect 4*H*-SiC supercell and defective supercell containing the $V_{Si}O_C$ center in charge state q, respectively; μ_O is the chemical potential of O atom in an O_2 molecule (because the oxygen ion implantation into 4*H*-SiC is a non-equilibrium process, the $V_{Si}O_C$ center is formed with oxygen atoms, hence the adoption of chemical potential of oxygen atom, which is more reasonable to our experiment); μ_{SiC} is the energy per SiC pairs which is calculated from a perfect 4*H*-SiC crystal; ε_F is the Fermi level, which is the band gap of the bulk 4*H*-SiC crystal; ε_v is the Fermi level reference to the valence band maximum of the bulk 4*H*-SiC, and ΔV is the potential alignment calculated from the difference of average potentials of supercell without and with the defect. The formation energies of vacancy defects centers in 4*H*-SiC with different charge states are plotted in Fig. 3. Comparing the defect formation energies of different vacancy defect centers, the $V_{Si}O_C$ center is the most stable in *n*-type 4*H*-SiC.

To understand the nature of $V_{Si}O_C$ centers in 4*H*-SiC, the density of state (DOS), optical and spin properties of the defect centers were calculated. The optimized $V_{Si}O_C$ centers with the charge state of $q = +2$, 0, -1 and -2 exhibit a perfect C_{3v} symmetry. Figure 4 shows the calculated DOS of the $V_{Si}O_C$ centers for the four charge states. According to the molecular orbitals (MOs) theory, the C_{3v} point group is formed by four sp^3 dangling bonds (DB) surrounding the Si vacancy. The $V_{Si}O_C$ center has two nondegenerate ($a$and v) and two-fold degenerated ($e_x$and e_y) MOs following the symmetries of the A_1 and E irreducible representations of C_{3v} point group [22, 23]. For the vacancy-related defect complex, these defect electronic states align in the order of $E_a < E_v < E_{e_x,e_y}$, and they can totally hold four spin-up (↑) and four spin-down (↓) DB electrons. For example, the $V_{Si}O_C^0$ center has six DB electrons so that two spin-polarized levels remain unoccupied. As shown the calculated DOS in Fig. 4b, all four majority-spin (↑) defect levels are occupied (one beneath the VBM and three in the band gap), while only two minority-spin (↓) defect levels are occupied. According to the DOS results, the Kohn–Sham eigenvalue associated with the $V_{Si}O_C^0$ center can be plotted (Fig. 5b). Similarly, the defect centers energy levels for the other charge states can be plotted, too (Fig. 5). The occupations of the defect levels shown in Figs. 4 and 5 determine the spin angular momenta (S) of different defect charge states. The net spin of the $V_{Si}O_c^q$ center is obtained as S = 0, 1, 1/2 and 0 for the charge state $q = +2$, 0, -1 and -2 ($q = +1$ is not stable in SiC), respectively. It is clear that the $V_{Si}O_c^0$ and

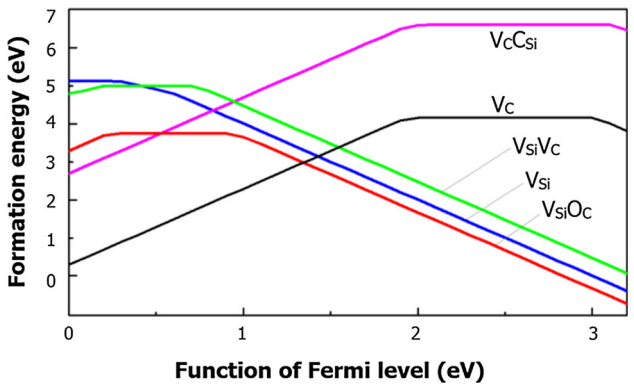

Fig. 3 (Color online) The calculated formation energies (E^f) as a function of Fermi level for single vacancies (V_C and V_{Si}), divacancy ($V_{Si}V_C$) and vacancy-impurity complex ($V_{Si}O_C$, V_CC_{Si}) in the oxygen ion-implanted 4*H*-SiC

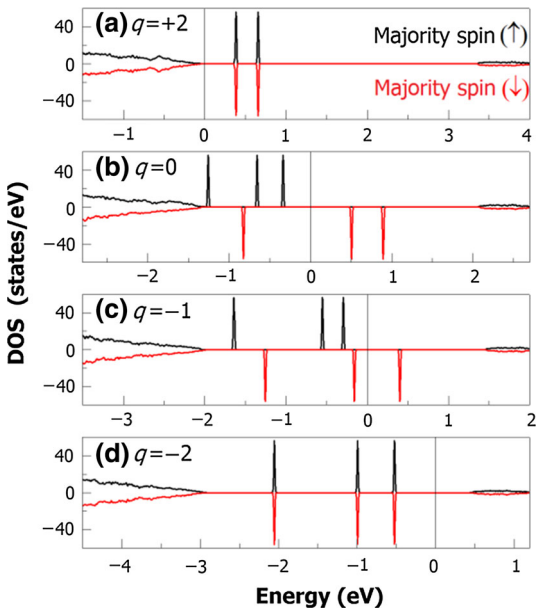

Fig. 4 (Color online) Calculated DOS for $V_{Si}O_C^q$ centers at different charge states in 4H-SiC. The energies are relative to the calculated chemical potentials ($E = 0$ eV) denoted by thin vertical lines

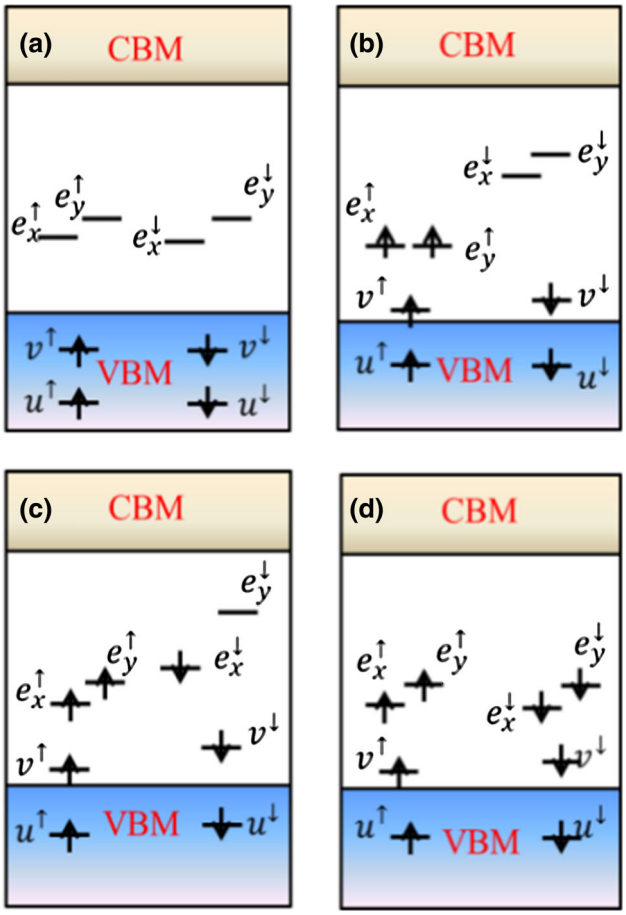

Fig. 5 (Color online) Schematic diagrams of defect energy levels of $V_{Si}O_C^q$ centers at different charge states in 4*H*-SiC, **a** $q = +2$ and $S = 0$, **b** $q = 0$ and $S = 1$, **c** $q = -1$ and $S = 1/2$ and **d** $q = -2$ and $S = 0$. Majority (minority) spins are denoted by *upward* (*downward*) *arrows*

$V_{Si}O_c^{-1}$ centers possess nonzero net spin, which can be reflected in ESR measurement.

In order to compare the ESR measurements, the *g* tensors of defect centers were calculated. Table 1 presents the calculated results of *g* tensors for vacancy defect centers in 4*H*-SiC. In 4*H*-SiC, there are two inequivalent sites (*k* stands for quasicubic position and *h* for quasihexagonal). The calculated *g* tensors of $V_{Si}(k)$, $V_C(h)$, $V_{Si}V_C(kh)$ and $V_CC_{Si}(hk)$ centers agree well with the measured *g* values, which all are close to the free electron value due to the absence of impurity atoms. But the calculated *g* tensors of $V_{Si}O_C(kh)$ centers are larger than the *g* tensor of the free electron due to introducing oxygen atoms. This can be found in the wavefunctions of $V_{Si}O_C$ centers in 4*H*-SiC. Figure 6 shows the minority-spin *v* and e_x states. From the minority-spin e_x state of $V_{Si}O_C^0$ and $V_{Si}O_c^{-1}$ centers (Fig. 6a, c, respectively), a small part of the density of the unpaired electrons is found at the oxygen atom. The similarity of the *g* values of the $V_{Si}O_C^0$ and $V_{Si}O_c^{-1}$ centers in 4*H*-SiC might be surprising. However, as shown in Fig. 6, the magnetization density is mainly localized at the carbon dangling bonds of the V_{Si} component of the defect pair, and the wavefunctions distribution of $V_{Si}O_C^0$ and $V_{Si}O_c^{-1}$ centers are similar. Thus, the similar *g* values of $V_{Si}O_C^0$ and $V_{Si}O_c^{-1}$ centers are reasonable. From the *g* tensors calculation, ESR signals of the oxygen ion implantation 4*H*-SiC may be attributed to the $V_{Si}O_C$ centers.

Because the ZPL values of the oxygen ion-implanted 4*H*-SiC are different from those of the present defect types, the spin-conserved optical transitions of $V_{Si}O_C$ centers in 4*H*-SiC were calculated. Theoretically, the spin-conserved optical transition of defect states can be approximated by Franck–Condon principle, so the total energy of the two electronic states was calculated using the constrained DFT approach. For example, the neutral $V_{Si}O_C$ center, there are six electrons to be accommodated in the orbitals. The ground-state configuration $a_u^2 a_v^2 e_{x,y}^2$ gives rise to the many-

Table 1 Measured and calculated values of the *g* tensor for the defect centers in 4*H*-SiC. The experimental values from Ref. [7, 15, 16]

Models	g_{xx}	g_{yy}	g_{zz}	Measured
V_{Si}^{-1} (*k*)	2.0046	2.0046	2.0043	2.0034
V_C^{+} (h)	2.0038	2.0036	2.0038	2.0038
V_C^{-1} (h)	2.0022	2.0022	2.0021	2.0028
$V_{Si}O_C^{-1}$ (kh)	2.0031	2.0052	2.0057	2.0053
$V_{Si}O_C^{0}$ (kh)	2.0059	2.0079	2.0048	2.0053
$V_{Si}V_C^{0}$ (kh)	2.0022	2.0022	2.0022	2.0023
$V_CC_{Si}^{0}$ (hk)	2.0021	2.0021	2.0021	2.0032

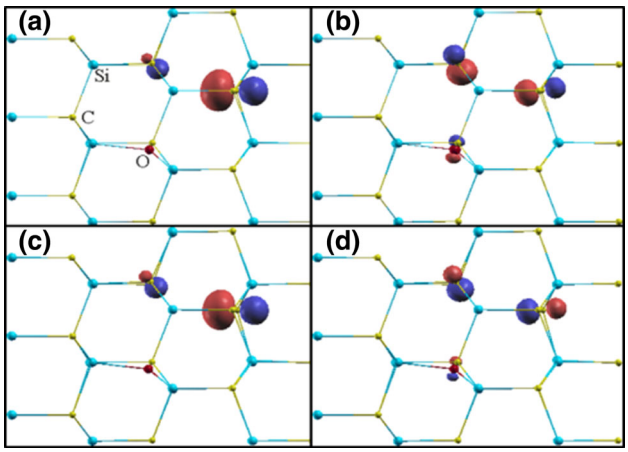

Fig. 6 (Color online) Charge density plots of minority-spin e_x (**a**) and *v* (**b**) defect states for $V_{Si}O_C^0$ center. Charge density plots of minority-spin e_x (**c**) and *v* (**d**) defect states for $V_{Si}O_C^{-1}$ center. *Red*, *yellow* and *blue* balls denote the oxygen, carbon and silicon atoms, respectively

electron state $^3A_2$. Promoting an electron from a singlet to the doublet gives the excited-state configuration $a_u^2 a_v^1 e_{x,y}^3$ and the many-electron state ^3E [23, 24]. The potential energy surfaces (PES) were the difference between the ground and excited states. The lowest PES of excited-state and ground-state transition was resulted in the ZPL. The calculated results are plotted in Fig. 7. The spin-conserved optical transition of $V_{Si}O_C^0(kh)$ center vertical absorption, vertical emission and ZPL is 1.06, 0.94 and 1.05 eV, respectively. However, the vertical absorption, vertical emission and ZPL of $V_{Si}O_c^{-1}(kh)$ center are 1.55, 1.39 and 1.45 eV, respectively. The ZPLs of defect centers with different inequivalent configurations in 4*H*-SiC have only small difference ($\sim$0.1 eV) [3, 6, 19]. The calculated ZPLs of $V_{Si}O_c^{-1}(kh)$ center are close to our experimental PL signatures. Combining the measurement and calculation results, the oxygen ion implantation produces oxygen-vacancy complex in 4*H*-SiC.

The calculation of spin-conserved optical transition of $V_{Si}O_C^0$ and $V_{Si}O_c^{-1}$ centers in 4*H*-SiC indicates that they are optically addressable. Therefore, some excellent properties suitable for qubit application are expected. As a spin qubit operation, the spin coherent property of defects is important for spin coherent manipulation. The electron spin coherence times of the $V_{Si}O_C^0$ and $V_{Si}O_c^{-1}$ centers in 4*H*-SiC can be calculated by the mean-field theory and first-principles calculations. The spin coherence is mainly effected by the interaction between electronic spin and nuclear spins, which is expressed as [17, 25],

$$\Delta E_{\text{hyp}} = \sum_n A_H \Delta N_n I_n \cdot s,$$

where A_H is the hyperfine coupling constant, ΔN_n is the fraction of the Fermi contact interaction of the defect electron with the nth nucleus, I_n is the nth nucleus spin in the supercell and $\boldsymbol{s}$ is the electron spin for defect. The spin operators I_n and $\boldsymbol{s}$ can be replaced by their average values in the mean-field approximation, i.e., $s = 1/2$ and $\bar{I}_n = \sum_i \alpha^i I_n^i$, where I_n^i and α^i are the ith isotopes of the nth nucleus nuclear spin and the corresponding of natural proportion. Knowing the hyperfine interaction energy, the electron spin coherence time can be estimated by the uncertainty principle at $T = 0$ K, i.e., $\Delta\tau = \hbar/2\Delta E_{\text{hyp}}$, where the $\hbar = 6.58 \times 10^{-16}$ eV s is the Planck's constant. Combined with the primary atomic orbitals of Si 2 s, O 2 s and C 2 s and corresponding LCPAO coefficients, the spin coherence times $\Delta\tau$ of the $V_{Si}O_C^0$ and $V_{Si}O_c^{-1}$ centers are calculated at 0.6 and 0.51 s, respectively. Such long spin coherence times of $V_{Si}O_C^0$ and $V_{Si}O_c^{-1}$ centers make them promising for a spin coherent manipulation and qubit operation in 4*H*-SiC.

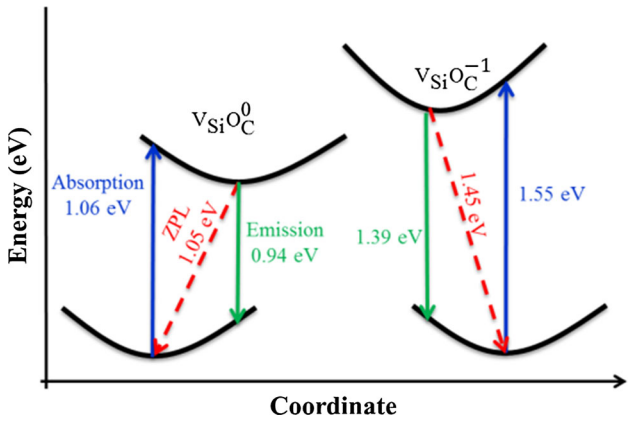

Fig. 7 (Color online) Configuration coordinate diagrams for neutral and negatively charged state $V_{Si}O_C$ centers in 4*H*-SiC. Absorption, emission and ZPL transitions are indicated along with their energies

4 Conclusion

In summary, oxygen ion-implanted 4*H*-SiC was investigated by ESR, PL and theoretical calculations. Combined the experimental results with first-principles calculations, we suggest that the oxygen-vacancy complex was the main defect in the oxygen ion-implanted 4*H*-SiC. The calculated defects formation energies of vacancy-type defect are shown that the $V_{Si}O_C$ centers were the most stable vacancy defect in *n*-type 4*H*-SiC. And then, the calculated *g* tensors and ZPL values of the $V_{Si}O_C$ centers are close to the ESR and PL experiment results. According to the PL experiment and ZPLs calculation, the $V_{Si}O_C^0$ and $V_{Si}O_c^{-1}$ centers are optically addressable. Finally, the spin coherence times of the $V_{Si}O_C^0$ and $V_{Si}O_c^{-1}$ centers show that oxygen ion-implanted 4*H*-SiC is a promising system for qubit application.

References

1. J.R. Weber, W.F. Koehl, J.B. Varley et al., Quantum computing with defects. Proc. Natl. Acad. Sci. USA **107**, 8513–8518 (2010). doi:10.1073/pnas.1003052107
2. P. Neumann, N. Mizuochi, F. Rempp et al., Multipartite entanglement among single spins in diamond. Science **320**, 1326–1329 (2008). doi:10.1126/science.1157233
3. A.L. Falk, B.B. Buckley, G. Calusine et al., Polytype control of spin qubits in silicon carbide. Nat. Commun. **4**, 1819 (2013). doi:10.1038/ncomms2854
4. L.P. Yang, C. Burk, M. Widmann et al., Electron spin decoherence in silicon carbide nuclear spin bath. Phys. Rev. B **90**, 241203 (2014). doi:10.1103/PhysRevB.90.241203
5. P.G. Baranov, A.P. Bundakova, A.A. Soltamova et al., Silicon vacancy in SiC as a promising quantum system for single-defect and single-photon spectroscopy. Phys. Rev. B **83**, 125203 (2011). doi:10.1103/PhysRevB.83.125203

6. K. Szász, V. Ivády, I.A. Abrikosov et al., Spin and photophysics of carbon-antisite vacancy defect in 4*H* silicon carbide: a potential quantum bit. Phys. Rev. B **91**, 121201 (2015). doi:10.1103/PhysRevB.91.121201
7. H.J. von Bardeleben, J.L. Cantin, E. Rauls et al., Identification and magneto-optical properties of the NV center in 4H-SiC. Phys. Rev. B **92**, 064104 (2015). doi:10.1103/Physrevb.92.064104
8. M. Ishimaru, R.M. Dickerson, K.E. Sickafus, High-dose oxygen ion implantation into 6*H*-SiC. Appl. Phys. Lett. **75**, 352–354 (1999). doi:10.1063/1.124372
9. A. Uedono, S. Tanigawa, T. Ohshima et al., Oxygen-related defects in O^+-implanted 6*H*-SiC studied by a monoenergetic positron beam. J. Appl. Phys. **86**, 5392–5398 (1999). doi:10.1063/1.371536
10. T. Ozaki, Variationally optimized atomic orbitals for large-scale electronic structures. Phys. Rev. B **67**, 155108 (2003). doi:10.1103/Physrevb.67.155108
11. N. Troullier, J.L. Martins, Efficient pseudopotentials for plane-wave calculations. Phys. Rev. B **43**, 1993–2006 (1991). doi:10.1103/PhysRevB.43.1993
12. P. Giannozzi, S. Baroni, N. Bonini et al., QUANTUM ESPRESSO: a modular and open-source software project for quantum simulations of materials. J. Phys.: Condens. Matter **21**, 395502 (2009). doi:10.1088/0953-8984/21/39/395502
13. J. Heyd, G.E. Scuseria, M. Ernzerhof, Hybrid functionals based on a screened Coulomb potential. J. Chem. Phys. **118**, 8207–8215 (2003). doi:10.1063/1.1564060
14. A. Gali, E. Janzen, P. Deak et al., Theory of spin-conserving excitation of the NV^- center in diamond. Phys. Rev. Lett. **103**, 186404 (2009). doi:10.1103/Physrevlett.103.186404
15. N.T. Son, P.N. Hai, E. Janzen, Silicon antisite in 4H SiC. Phys. Rev. Lett. **87**, 045502 (2001). doi:10.1103/PhysRevLett.87.045502
16. N.T. Son, X.T. Trinh, L.S. Lovlie et al., Negative-U system of carbon vacancy in 4H-SiC. Phys. Rev. Lett. **109**, 187603 (2012). doi:10.1103/Physrevlett.109.187603
17. Y.G. Zhang, Z. Tang, X.G. Zhao et al., A neutral oxygen-vacancy center in diamond: a plausible qubit candidate and its spintronic and electronic properties. Appl. Phys. Lett. **105**, 052107 (2014). doi:10.1063/1.4892654
18. N.T. Son, A. Henry, J. Isoya et al., Electron paramagnetic resonance and theoretical studies of shallow phosphorous centers in3C-, 4H-, and 6H-SiC. Phys. Rev. B **73**, 075201 (2006). doi:10.1103/PhysRevB.73.075201
19. L. Gordon, A. Janotti, C.G. Van de Walle, Defects as qubits in 3*C*- and 4*H*-SiC. Phys. Rev. B **92**, 045208 (2015). doi:10.1103/Physrevb.92.045208
20. S. Arpiainen, K. Saarinen, P. Hautojarvi et al., Optical transitions of the silicon vacancy in 6H-SiC studied by positron annihilation spectroscopy. Phys. Rev. B **66**, 075206 (2002). doi:10.1103/Physrevb.66.075206
21. C.G. Van de Walle, J. Neugebauer, First-principles calculations for defects and impurities: applications to III-nitrides. J. Appl. Phys. **95**, 3851–3879 (2004). doi:10.1063/1.1682673
22. A. Lenef, S.C. Rand, Electronic structure of the N-*V* center in diamond: theory. Phys. Rev. B **53**, 13441–13455 (1996). doi:10.1103/PhysRevB.53.13441
23. J.A. Larsson, P. Delaney, Electronic structure of the nitrogen-vacancy center in diamond from first-principles theory. Phys. Rev. B **77**, 165201 (2008). doi:10.1103/Physrevb.77.165201
24. F.M. Hossain, M.W. Doherty, H.F. Wilson et al., Ab initio electronic and optical properties of the NV^{-1} center in diamond. Phys. Rev. Lett. **101**, 226403 (2008). doi:10.1103/Physrevlett.101.226403
25. Y. Tu, Z. Tang, X.G. Zhao et al., A paramagnetic neutral $V_{Al}O_N$ center in wurtzite AlN for spin qubit application. Appl. Phys. Lett. **103**, 072103 (2013). doi:10.1063/1.4818659